Journal of the Optical Society of Korea, Vol 5, No. 1, March 2001, pp. 20-24

Measurement of Zero Dispersion Wavelength in an Optical Fiber Using the Oscillatory Behavior of Four-Wave Mixing Efficiency

Dong Hwan Kim*, Sang Hyuck Kim, Jae Cheol Jo, and Sang Sam Choi

Photonics Research Center, Korea Institute of Science and Technology, Seoul 130-650, KOREA

(Received August 23, 2000)

Non-destructive measurement of zero-dispersion wavelength variation in a dispersion shifted fiber by four-wave mixing technique is carried out. The oscillatory behavior of the four-wave mixing efficiency is utilized for the measurement of the linear dispersion slope and zero-dispersion wavelength. A simple formula useful for engineering estimation of the characteristics of fiber four-wave mixing efficiency is presented.

OCIS codes : 060.0060, 060.2400, 300.0030, 300.6290.

I. INTRODUCTION

Four-wave mixing (FWM) is one of the interesting non-linearities such as optical phase conjugation and wavelength converter in optical fibers [1,2] and semiconductor optical amplifiers (SOA) [3,4]. Recently, several studies have been reported on nondestructive measurement techniques for distribution of chromatic dispersion wavelengths in dispersion shifted fibers (DSF) because management of fiber dispersion would be the key for WDM optical transmission systems [5–7]. FWM phenomena in an optical fiber or SOA as a wavelength converter are used for ultra-high speed optical signal processing [8–10]. Compared with SOA-FWM, optical fibers have the parametric nonlinear phenomenon of the optical Kerr effect, which has low phase noise.

Therefore, FWM in the optical fiber is used in low phase-noise clock extraction or in all-optical demultiplexing system [11,12], but it is also harmful in the WDM transmission system because of the new frequency generation. It is necessary to determine the channel frequency separation at the operating wavelength of the WDM system to prevent optical degradation of the transmitting signals. For a system transmitting more than three channel carriers, cross-talk due to FWM must be avoided in the system design. To solve the problem, it is important to consider the generated wavelength efficiency with respect to the phase mismatch in the FWM process for arbitrary input signal power and wavelength separation. The efficiency of the newly generated waves in the FWM process depends on the channel frequency separation, fiber-chromatic dispersion, and fiber length.

In this paper, we focus the oscillatory behavior of the FWM efficiency with the phase mismatching parameters. The dependence of FWM efficiency on the frequency separation has been investigated in dispersion-shifted fibers. We deduced the linear dispersion slope near the zero dispersion wavelength region from the oscillatory behavior of the FWM efficiency with frequency separation.

II. THEORY

FWM is easily observed in optical fibers for all low input powers and the low nonlinear coefficients because optical fiber has small core size and long interaction length. However, in order to generate an efficient FWM light, a proper phase matching should be considered. Since phase mismatch comes from the different group velocities of the different wavelengths, symmetrical configuration of the input wavelength arrangement is needed. When three waves of frequencies f_i, f_j, f_k ($f_i = f_j$) are incident on the optical fiber, the new frequency component of $f_{ijk} = f_i + f_j - f_k$ (subscripts i, j and k select 1,2 and 3) are generated due to the third order nonlinear polarization. In Fig. 1(a), nine new generated frequencies f_{ijk} are indicated. Then, if the frequency separation is equal ($\Delta f = f_2 - f_1 = f_3 - f_2$), the three signal frequencies coincide with newly generated frequencies. This leads to the cross-talk problem in wavelength multiplexed communication systems. The time-averaged optical

power $P_{ijk}(L, \Delta\beta)$ through the FWM process for f_{ijk} is as

$$P_{ijk}(L,\Delta\beta) = \frac{1024\pi^6}{n^4\lambda^2c^2}(D\chi_{1111})^2\frac{P_i(0)P_j(0)P_k(0)}{A_{eff}^2} \times e^{-\alpha L}\frac{(1-e^{-\alpha L})^2}{\alpha^2}\eta, \quad (1)$$

where P_i, P_j, and P_k are the input light powers of f_i, f_j, and f_k, n is the fiber refractive index, λ is wavelength, c is light velocity in vacuum, A_{eff} is the effective mode area of the fiber, α is fiber loss coefficient, and D is the degeneracy factor, and χ_{1111} is the third-order nonlinear susceptibility. η represents the dependence of the FWM efficiency on the phase mismatching, $\Delta\beta = \beta(f_i) + \beta(f_j) - \beta(f_k) - \beta(f_{ijk})$, which is written as

$$\eta = \frac{\alpha^2}{\alpha^2+\Delta\beta^2}\left[1+\frac{4e^{-\alpha L}\sin^2(\Delta\beta L/2)}{(1-e^{-\alpha L})^2}\right], \quad (2)$$

where β is the propagation constant and can be approximately expressed at around the zero-dispersion wavelength as

$$\beta(f_i) = \beta(f_o) + (f_i - f_o)\frac{d\beta}{df}(f_o) + \frac{1}{2}(f_i-f_o)^2 \times\frac{d^2\beta}{df^2}(f_o) + \frac{1}{6}(f_i-f_o)^3\frac{d^3\beta}{df^3}(f_o) \quad (3)$$

The above expression can be rewritten using the fiber chromatic dispersion D_c and the relation $D_c(f_c) = 0$, as

$$\beta(f_i) = \beta(f_o) + (f_i - f_o)\frac{d\beta}{df}(f_o) + (f_i-f_o)^2\frac{\pi\lambda^4}{3c^2}\frac{dD_c}{d\lambda} \quad (4)$$

Therefore, the propagation constant difference is

$$\Delta\beta = -\frac{\lambda^4\pi}{c^2}\frac{dD_c}{d\lambda}(f_i-f_o) + (f_j-f_o) \times(f_i-f_k)(f_j-f_k), \quad (5)$$

Eq. (5) describes the phase-mismatching in the zero-dispersion wavelength. It is noted that the FWM efficiency reaches 1 as $\Delta\beta = 0$. The phase matching condition is always satisfied when the zero dispersion wavelength is positioned at the middle between two lights of f_i and f_j. In particular, in the case of the partially degenerate frequencies ($f_i = f_j$), the phase matching condition is always satisfied when f_i coincides with the zero-dispersion wavelength. Thus, FWM light is generated at the side opposite to the f_k frequency light wavelength with the zero-dispersion wavelength as the center point (Fig.1(b)). When the fiber loss (α) is assumed negligible, the FWM efficiency, Eq. (2) is expressed as

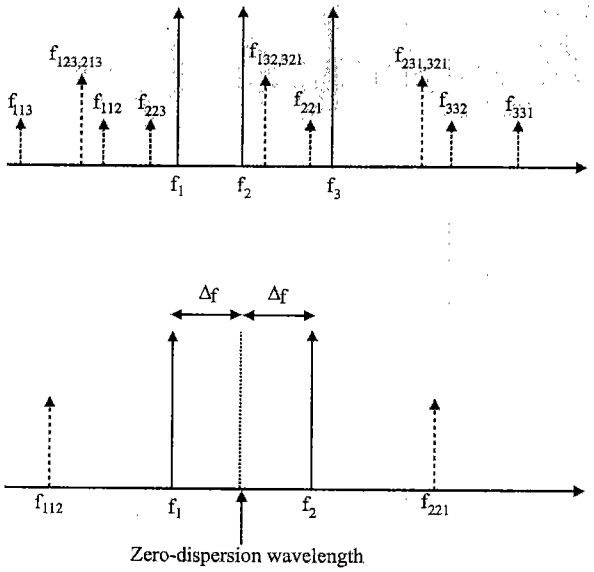

FIG. 1. Sketch of the three input waves and nine waves generated through the four-wave mixing process, (a), and the two input waves (partially degenerate FWM) and generated FWM frequency (b).

$$\begin{aligned}\eta &= \frac{\alpha^2}{\alpha^2+\Delta\beta^2}\left[1+\frac{4e^{-\alpha L}\sin^2(\Delta\beta L/2)}{(1-e^{-\alpha L})^2}\right]\\ &\simeq \frac{\alpha^2}{\Delta\beta^2}\left[1+\frac{(1-\alpha L)\sin^2(\Delta\beta L/2)}{\left(\frac{\alpha L}{2}\right)^2}\right]\\ &\simeq \frac{(1-\alpha L)\sin^2(\Delta\beta L/2)}{\Delta\beta^2\left(\frac{L}{2}\right)^2}\\ &\simeq \frac{\sin^2(\Delta\beta L/2)}{(\Delta\beta L/2)^2}\end{aligned} \quad (6)$$

Eq. (6) describes the oscillating behavior with the phase mismatch. The first minimum of the FWM light occurs at the $(\Delta\beta)_\pi L/2 = \pi$. With the expression of the propagation constant difference (5), the linear slope of the dispersion can be deduced as [13].

$$\frac{dD_c}{d\lambda} = \frac{1}{cL\lambda_F^4\left(\frac{1}{\lambda_\pi}-\frac{1}{\lambda_k}\right)^2\left(\frac{1}{\lambda_\pi}-\frac{1}{\lambda_o}\right)}, \quad \frac{1}{\lambda_F} = \frac{2}{\lambda_\pi} - \frac{1}{\lambda_k} \quad (7)$$

where λ_F is the newly generated FWM wavelength, λ_o is the zero-dispersion wavelength, and λ_π is the degenerate wavelength ($\lambda_i = \lambda_j$) at which the first minimum FWM efficiency occurs. Therefore, we can

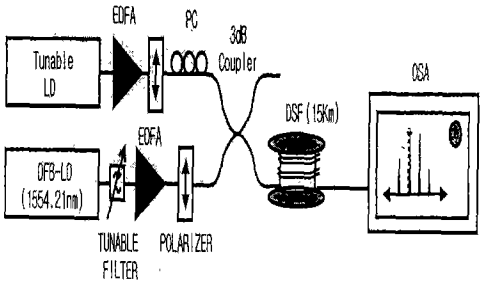

FIG. 2. Experimental setup for FWM. PC; Polarization Controller, DSF; Dispersion Shifted Fiber, OSA; Optical Spectrum Analyzer.

get the linear dispersion curve near the zero-dispersion wavelength as

$$D_c(\lambda) = \left(\frac{dD_c}{d\lambda}\right)(\lambda - \lambda_o) \qquad (8)$$

III. EXPERIMENT AND RESULTS

Experiments were carried out to study a fiber FWM in the zero-dispersion wavelength region. Degenerate FWM was investigated where two of three input lights were identical. For measurements of the FWM characteristics, 15km-long dispersion shifted fiber (DSF) and 30km-long DSF were used. The experimental setup is shown in Fig. 2. A tunable pump light (λ_i) and DFB LD probe light (λ_k = 1554.21 nm) were combined by a fiber coupler after each amplification through an EDFA and were launched in the dispersion shifted fiber. The launched input power was about

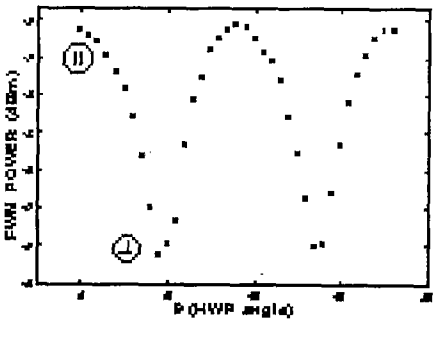

FIG. 3. Polarization dependence of FWM process. θ is the rotation angle of the half wave plate, which the angle between the input polarization states is 2θ.

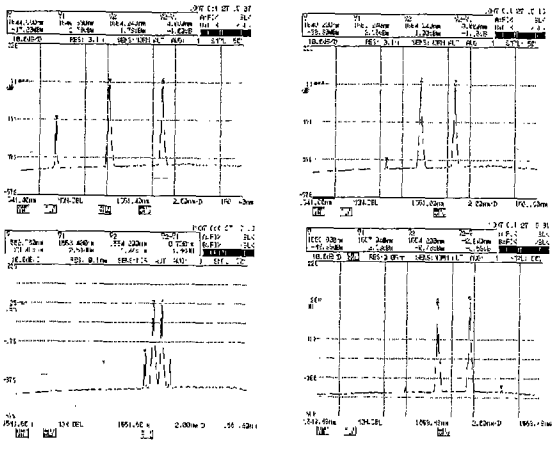

FIG. 4. Optical spectra of the partially degenerate FWM process as the pump light is scanned around the zero dispersion wavelength with the probe wave fixed at the 1554.2nm; (a) pump wave=1549.56nm, left FWM wave = 1554.88nm, (b) pump wave=1549.56nm, left FWM wave=1548.22nm (c) pump wave=1549.56nm, left FWM wave=1552.76nm, right FWM wave=1554.92nm (d) pump wave=1549.56nm.

6 dBm for each.

FWM power variation was measured with espect to the polarization state by a rotating half wave plate before the fiber coupler. Fig. 3 shows the maximum FWM power was obtained at the parallel polarization state because the maximum power period is 180 degrees. When the half wave plate ($\lambda/2$-plate) is θ, the polarization states of the two input light waves have the angle of 2θ. Therefore, the period of 90 degrees of half plate angle in Fig. 3 means the power period of 180 degrees, which is parallel.

As the pump light is swept from 1549.56nm to 1557.04nm, FWM spectra, from (a) to (d), are investigated in Fig. 4. When the pump light is near the zero- dispersion wavelength(1549.5nm), the phase-mismatch of left FWM component is nearly zero from Eq. (5). Whereas the phase-mismatch of the right FWM component is far from zero. Therefore, the left FWM component near the zero-dispersion wavelength dominates over the right component. When the pump wave is close to the probe wave in Fig. 4(c), the nearly degenerate FWM occurs. Therefore, both of the left and right FWM components are observed. In Fig. 4(d), when the two input waves (pump wavelength=1557.04nm, probe wavelength=1554.2nm) are far from the zero-dispersion wavelength, both of the FWM frequency components disappear because of the large phase mismatch.

If the FWM efficiency is defined as the power ratio

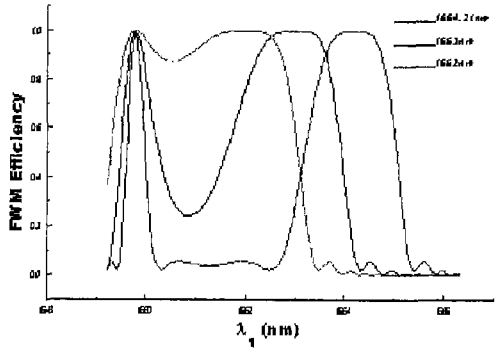

FIG. 5. Calculation result of FWM efficiency curve as a function of the scanning pump wavelength, Here, the probe wavelengths are 1554.21nm, 1553nm, and 1552nm.

of the FWM light to input probe light as $P(L, f_{ijk})/P(0, f_k)$, FWM efficiency curve with the scanning pump light wavelength is calculated in Fig. 5. From the result, two maximum efficiency points are shown. One is at the zero-dispersion wavelength and the other is at the probe light wavelength. Around the probe light wavelength, the efficiency has broader bandwidth than at the zero-dispersion wavelength because the degenerate FWM occurs at the probe light wavelength.

In order to find 3dB bandwidth of the FWM process, the probe light was scanned with the pump wave fixed at the zero-dispersion wavelength (1549.5nm). 3dB bandwidth was found to be 20nm in Fig. 6, which is very wide compared with the SOA-FWM.

FWM efficiency curve as a function of the tuning pump wavelength is measured with an optical spectrum analyzer of 0.05nm resolution in Fig. 7(a). The probe wavelength is fixed at the 1554.21nm. In the experimental results, two peak efficiencies are clearly shown at the zero-dispersion wavelength and probe wavelength, which are both phase matched. The wider bandwidth at the probe wavelength is expected from the smaller phase mismatching because it has square dependence on $(f_i - f_k)$ and linear dependence on $(f_i - f_o)$. The oscillating behavior of FWM efficiency was investigated by fine tuning the pump wavelength near the zero dispersion wavelength in Fig. 7(b). This experiment can also be applied for measuring the zero-dispersion wavelength because the zero-dispersion wavelength cannot be known at first. The efficiency shows damped oscillatory behavior as phase-mismatch increases. Since the first minimal efficiency appears approximately in the condition of $(\Delta\beta)_\pi L/2 = \pi$ in Eq. (6), the dispersion slope near the zero-dispersion wavelength can be calculated. The measured slope was 0.069ps/km·nm·nm, which is reasonable with the value of 0.075 ps/km·nm·nm mea-

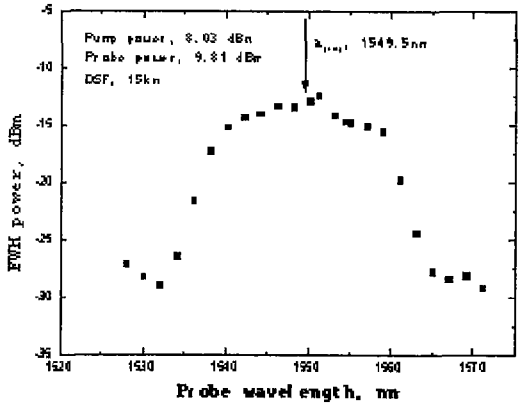

FIG. 6. FWM power as a probe wavelength with the pump wave fixed at the zero-dispersion wavelength. 3dB bandwidth of the fiber FWM is found to be 20nm.

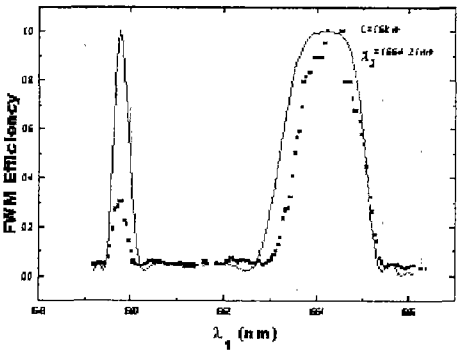

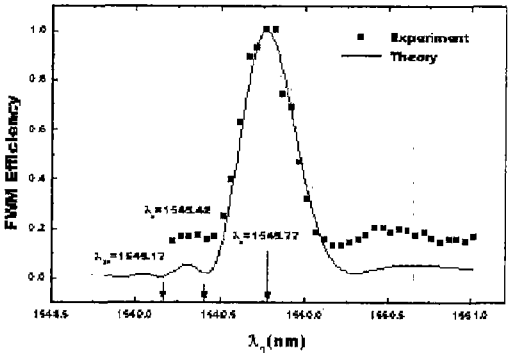

FIG. 7. FWM efficiency as a pump wavelength (λ_1) near the zero-dispersion wavelength. Probe wavelength (λ_2) is set at 1554.21nm and the fiber length is 15Km long (a). Oscillatory FWM efficiency behavior (b). The solid line is a calculation result.

sured by the conventional chromatic dispersion analyzer.

The same experiment was carried out for 30km-long DSF for which two 15km-long DSFs are connected. The dispersion slope was measured as 0.048 ps/km·nm·nm. The reason, as Inoue pointed out [2], is that a real fiber consists of many fiber segments with slightly different zero-dispersion wavelengths. Therefore, the phase matching condition cannot be completely satisfied. As the fiber length increases, the zero-dispersion wavelength deviates widely because of the non-uniformity of the fiber core size. This leads the large phase-mismatch and the oscillatory period of the FWM efficiency to be reduced, which makes it difficult to find the first minimal FWM efficiency point.

IV. CONCLUSIONS

Four-wave mixing experiments in an optical fiber are carried out. New application for measuring the linear dispersion slope in dispersion-shifted fibers is proposed by the four-wave mixing efficiency curve as a pump light is scanned near the zero dispersion wavelength. The measured dispersion slope was reasonable compared with the conventional method. The deviation of the zero dispersion wavelength along the fiber length plays an important role in the FWM behavior and should be evaluated by the statistical analysis because of non-uniformity of the fiber core size.

*Corresponding author : dhwan@kist.re.kr.

REFERENCES

[1] K. O. Hill, D. C. Johnson, B. S. Kawasaki, and R. I. MacDonald, J. Appl. Phys. **49**, 5098 (1978).
[2] K. Inoue and H. Toba, IEEE Photon. Technol. Lett. **4**, 69 (1992).
[3] T. Ducellier, M. B. Bibey, IEEE Photon. Technol. Lett. **8**, 530 (1996).
[4] F. Favre and D. L. Guen, IEEE J. Quantum Elec. **26**, 858 (1990).
[5] H. Onaka, K. Otsuka, H. Miyata, and T. Chikama, IEEE Photon. Technol. Lett. **6**, 1454 (1994).
[6] Y. Suetsugu, T. Kato, T. Okuno, and M. Nishimura, IEEE Photon. Technol. Lett. **7**, 1459 (1995).
[7] M. Eiselt, R. M. Jopson, and R. H. Stolen, J. Lightwave Technol. **15**, 135 (1997).
[8] M. W. Maeda, W. B. Sessa, W. I. Way, A. Y. Yan, L. Curtis, R. Spicer, and R. I. Laming, J. of Lightwave. Technol. **8**, 1402 (1990).
[9] T. Saito, Y. Yano, N. Henmi, in OFC'94, Tech. Digest, TuN3 (1994).
[10] O. Kamatani and S. Kawanishi, J. Lightwave Technol. **14**, 1757 (1996).
[11] P. A. Andrekson, N. A. Olsson, J. R. Simpson, T. Tanbun-Ek, R. A. Logan and M. Haner, Electron. Lett. **27**, 922 (1991).
[12] T. Morioka, S. Kawanishi, K. Uchiyama, H. Takara, and M. Saruwatari, Electron. Lett. **30**, 591 (1994).
[13] D. H. Kim, S. H. Kim, J. C. Jo, S. K. Kim, S. S. Choi, in Nonlinear Optics'98, (Kauai, USA, 1998) 168.